

# First application of mass measurement with the Rare-RI Ring reveals the solar $r$ -process abundance trend at $A = 122$ and $A = 123$

H. F. Li,<sup>1,2,3,4</sup> S. Naimi,<sup>3,\*</sup> T. M. Sprouse,<sup>5</sup> M. R. Mumpower,<sup>5</sup> Y. Abe,<sup>3</sup> Y. Yamaguchi,<sup>3</sup> D. Nagae,<sup>3,†</sup> F. Suzuki,<sup>3,‡</sup> M. Wakasugi,<sup>3</sup> H. Arakawa,<sup>6</sup> W.B. Dou,<sup>6</sup> D. Hamakawa,<sup>6</sup> S. Hosoi,<sup>6</sup> Y. Inada,<sup>6</sup> D. Kajiki,<sup>6</sup> T. Kobayashi,<sup>6</sup> M. Sakaue,<sup>6</sup> Y. Yokoda,<sup>6</sup> T. Yamaguchi,<sup>6</sup> R. Kagesawa,<sup>7</sup> D. Kamioka,<sup>7</sup> T. Moriguchi,<sup>7</sup> M. Mukai,<sup>7,§</sup> A. Ozawa,<sup>7</sup> S. Ota,<sup>8,¶</sup> N. Kitamura,<sup>8</sup> S. Masuoka,<sup>8</sup> S. Michimasa,<sup>8</sup> H. Baba,<sup>3</sup> N. Fukuda,<sup>3</sup> Y. Shimizu,<sup>3</sup> H. Suzuki,<sup>3</sup> H. Takeda,<sup>3</sup> D.S. Ahn,<sup>3,9</sup> M. Wang,<sup>1</sup> C.Y. Fu,<sup>1</sup> Q. Wang,<sup>1</sup> S. Suzuki,<sup>1</sup> Z. Ge,<sup>1,\*\*</sup> Yu. A. Litvinov,<sup>10</sup> G. Lorusso,<sup>11,12</sup> P. M. Walker,<sup>12</sup> Zs. Podolyak,<sup>12</sup> and T. Uesaka<sup>3</sup>

<sup>1</sup>*Institute of Modern Physics, Chinese Academy of Sciences, Lanzhou 730000, People's Republic of China*

<sup>2</sup>*Lanzhou University, Lanzhou 730000, People's Republic of China*

<sup>3</sup>*RIKEN Nishina Center, RIKEN, Saitama 351-0198, Japan*

<sup>4</sup>*University of Chinese Academy of Sciences, Beijing 100049, People's Republic of China*

<sup>5</sup>*Theoretical Division, Los Alamos National Laboratory, Los Alamos, New Mexico, 87545, USA*

<sup>6</sup>*Department of Physics, Saitama University, Saitama 338-8570, Japan*

<sup>7</sup>*Institute of Physics, University of Tsukuba, Ibaraki 305-8571, Japan*

<sup>8</sup>*Center for Nuclear Study, University of Tokyo, Wako, Saitama 351-0198, Japan*

<sup>9</sup>*Center for Exotic Nuclear Studies, Institute for Basic Science (IBS), Daejeon 34126, Republic of Korea*

<sup>10</sup>*GSI Helmholtzzentrum für Schwerionenforschung, Planckstraße 1, 64291 Darmstadt, Germany*

<sup>11</sup>*National Physical Laboratory, Teddington, TW11 0LW, United Kingdom*

<sup>12</sup>*Department of Physics, University of Surrey, Guildford GU2 7XH, United Kingdom*

(Dated: December 13, 2021)

The Rare-RI Ring (R3) is a recently commissioned cyclotron-like storage ring mass spectrometer dedicated to mass measurements of exotic nuclei far from stability at Radioactive Isotope Beam Factory (RIBF) in RIKEN. The first application of mass measurement using the R3 mass spectrometer at RIBF is reported. Rare isotopes produced at RIBF,  $^{127}\text{Sn}$ ,  $^{126}\text{In}$ ,  $^{125}\text{Cd}$ ,  $^{124}\text{Ag}$ ,  $^{123}\text{Pd}$ , were injected in R3. Masses of  $^{126}\text{In}$ ,  $^{125}\text{Cd}$ , and  $^{123}\text{Pd}$  were measured and the mass uncertainty of  $^{123}\text{Pd}$  was improved. The impact of the new  $^{123}\text{Pd}$  result on the solar  $r$ -process abundances in a neutron star merger event is investigated by performing reaction network calculations of 20 trajectories with varying electron fraction  $Y_e$ . It is found that the neutron capture cross section on  $^{123}\text{Pd}$  increases by a factor of 2.2 and  $\beta$ -delayed neutron emission probability,  $P_{1n}$ , of  $^{123}\text{Rh}$  increases by 14%. The neutron capture cross section on  $^{122}\text{Pd}$  decreases by a factor of 2.6 leading to pileup of material at  $A = 122$ , thus reproducing the trend of the solar  $r$ -process abundances. Furthermore, the nuclear deformation predicted to reach its maximum before  $N = 82$  in the Pd isotopic chain is examined. The new mass measurement shows no evidence of such large deformation, though, experimental uncertainty should be further improved to draw a definitive conclusion. This is the first reported measurement with a new storage ring mass spectrometry technique realized at a heavy-ion cyclotron and employing individual injection of the pre-identified rare nuclei. The latter is essential for the future mass measurements of the rarest isotopes produced at RIBF.

The discovery of the historical GW170817 event of binary neutron stars merger and the subsequent kilonova AT2017go [1] for the GW170817 [2] was a major milestone toward revealing the secret of the synthesis of heavy elements via the rapid neutron capture process ( $r$ -process)[3]. The recent identification of strontium in the kilonova radiation gave a strong evidence of the produc-

tion of  $r$ -process elements [4]. However, modeling of the accretion disk formed in supernova-triggered collapse of rapidly rotating massive stars or collapsars, showed that  $r$ -process elements could be also produced in considerable amounts [5]. The presence of  $r$ -process heavy elements was also observed in the dwarf galaxy Reticulum II [6], where the accretion disk of collapsars might be the main source of production. Recent studies suggest that heavy elements might be synthesized in three different sites based on observations of low metallicity stars [7], characterized by three types of patterns, a weak  $r$ -process, a strong solar-type  $r$ -process, and an actinide boosted  $r$ -process. To model the formation of heavy chemical elements under different astrophysical conditions, a large and diverse amount of nuclear data is needed, especially for neutron-rich nuclei that live for a fraction of a second. Nuclear masses are important ingredients since they reflect the neutron separation energies, which are required

\* Corresponding author: snaimi(at)riken.jp

† Current affiliation: Research Center for SuperHeavy Elements, Kyushu University, Fukuoka, Fukuoka 819-0395, Japan

‡ Current affiliation: Advanced Science Research Center, Japan Atomic Energy Agency, Ibaraki 319-1195, Japan

§ Current affiliation: RIKEN Nishina Center, RIKEN, Saitama 351-0198, Japan

¶ Current affiliation: Research Center for Nuclear Physics, Osaka University, Osaka, 567-0047, Japan

\*\* Current affiliation: GSI Helmholtzzentrum für Schwerionenforschung, Planckstraße 1, 64291 Darmstadt, Germany

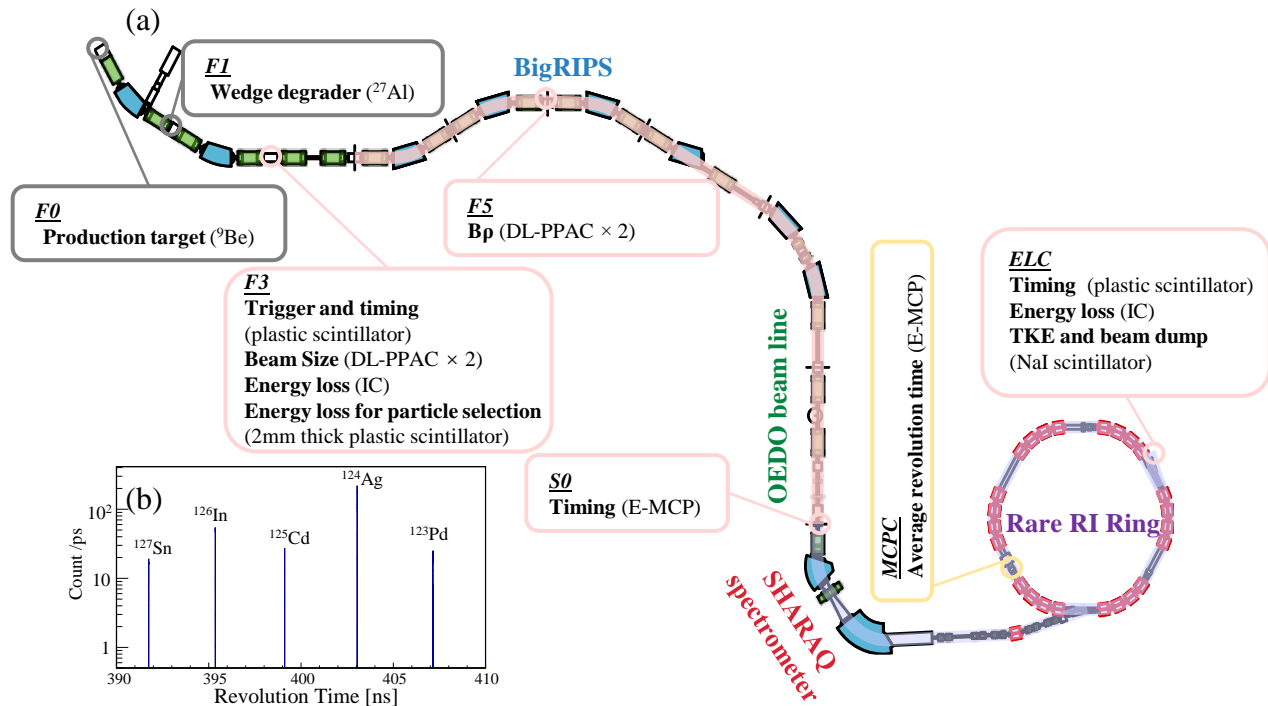


FIG. 1. (a) Configuration of the detectors installed in the beam line and Rare RI Ring (R3). (b) The revolution time spectrum for the 5 nuclei.

for the determination of neutron capture rates and photodissociation rates [3, 8, 9]. A vast number of neutron-rich nuclei involved in the  $r$ -process can now be produced in the laboratory at rare isotope facilities and their properties measured with high precision. However, all nuclei needed for modelling the  $r$ -process will not be accessible even at the new-generation radioactive-ion beam facilities. A robust model based on accurate properties of neutron-rich nuclei is thus essential to reveal the astrophysical conditions in which heavy elements could be produced. Such a model will help quantify the production rates in various sites, which will result in more accurate galactic chemical evolution calculations capable of reproducing the  $r$ -process elements' chemical abundances [10, 11].

This Letter reports precision mass measurements of neutron-rich nuclei produced at the Radioactive Isotope Beam Factory (RIBF) and their implication in the production of  $r$ -process elements with atomic mass number  $A=122$  and  $A=123$ . Mass measurements of nuclei with neutron number  $N=77$  were performed for the first time with a new type of mass spectrometer, namely the Rare-RI Ring (R3), recently commissioned at the RIBF/RIKEN facility [12]. We examine the implication of the  ${}^{123}\text{Pd}$  mass on the abundance calculation for a neutron star merger event. These first mass measurements at RIBF of neutron-rich isotopes in a remote region of the nuclear chart open a door to reaching  $r$ -process nuclei at  $N=82$  and beyond.

In the experiment, the secondary beam was produced

by in-flight-fission of the 345 MeV/u  ${}^{238}\text{U}$  beam provided by the Superconducting Ring Cyclotron (SRC) impinged on the 6 mm thick beryllium target which was placed upstream of the BigRIPS separator at F0 focal plane (see Fig. 1). The secondary fragments of interest were separated by the first stage of the BigRIPS as described in [13]. For this purpose, a 5 mm wedge-shaped degrader was introduced at the F1 focal plane of the BigRIPS. The magnetic rigidity  $B\rho$  and the transmission efficiency were optimized for the reference particle  ${}^{124}\text{Ag}$ . The momentum selection was done by setting the slits at F1 to  $\pm 2$  mm, corresponding to the R3 momentum acceptance of  $\pm 0.3\%$ . The injection kicker magnets system placed inside the R3 is limited to a repetition rate of 100 Hz. Therefore, to accept the quasi-continuous beam from the SRC, the individual self-injected trigger technique was developed for injecting pre-identified particles of interest [14]. The particle identification (PID) was achieved by the  $\Delta E$ -TOF method in the beam line, where  $\Delta E$  is the energy loss measured by the ionization chamber (IC) placed at F3 and TOF is the time-of-flight measured by the plastic scintillator at F3 and the E-MCP detector [15] at S0 of the SHARQA spectrometer. Also a 2-mm thick plastic scintillator was placed after the IC at F3 to get a rough  $\Delta E$  information needed for removing contaminations [16]. Two position monitors PPACs (Parallel Plate Avalanche Counter) were installed at F3 to monitor the beam size and two double PPACs were installed at F5 which is a dispersive focal plane to measure  $B\rho$  of every individual particle prior to its injection into the R3.

The particle circulates in the R3 for about 1800 revolutions before it is ejected from the ring. The total TOF in the R3 was measured by the E-MCP detector at S0 and a plastic scintillator detector placed at ELC after the ejection from the R3. Another IC was installed at ELC, where an additional PID was performed. Finally, particles were stopped in the NaI scintillator detector placed behind the IC at ELC.

The mass-to-charge ratio ( $m/q$ ) of the particle of interest with a revolution time  $T$  is determined relative to a reference particle with  $m_0/q_0$  and  $T_0$  by using the following formula [12, 17]:

$$\frac{m}{q} = \frac{m_0}{q_0} \frac{T}{T_0} \sqrt{\frac{1 - \beta^2}{1 - \left(\frac{T}{T_0}\beta^2\right)}}, \quad (1)$$

where  $\beta$  is the velocity of the particle of interest relative to the speed of the light in vacuum. Revolution time spectrum of all injected nuclei is shown in Fig. 1 (b) (details of determination of the revolution time in R3 can be found in [18]). Since the isochronous condition of the ring is optimized for the reference particle,  $T_0$  is independent of the momentum. To determine the mass, the velocity  $\beta$  needs to be determined event-by-event from the time-of-flight along the beamline from F3 to S0 ( $TOF_{3S0}$ ) by using the following equation,

$$\beta = \frac{Length_{3S0}}{(TOF_{3S0} + TOF_{offset})}. \quad (2)$$

The average path length from F3 to S0 ( $Length_{3S0}$ ) and the  $TOF_{offset}$  caused by the electronics and the energy loss in the detectors on the beamline, are determined via Eq.(2) by using known masses of  $^{124}\text{Ag}$  and  $^{127}\text{Sn}$ . The parameters that could reproduce the known  $m/q$  values are  $Length_{3S0} = 84.859(2)$  m and  $TOF_{offset} = 325.47(1)$  ns. The mass is then determined for each event via Eq.(1). Additional systematic uncertainties,  $\sigma_{sys}$ , due to the determination of parameters such as  $Length_{3S0}$ ,  $TOF_{offset}$  and  $T_0$  were estimated and reported in Table I. Details of data analysis method can be found in references [12, 18]. The full data analysis method as well as the details of estimating the systematic uncertainties will be reported in a subsequent publication. The mass excess values determined for all nuclei are listed in Table I. Comparison with literature values from the recent Atomic Mass Evaluation, AME2020 [19], are plotted in Fig. 2. As shown in Table I, the uncertainties are dominated by the mass uncertainty of the reference particle  $^{124}\text{Ag}$  at 250 keV. The choice of  $^{124}\text{Ag}$  as a reference instead of  $^{125}\text{Cd}$ , which has lower uncertainty, is mainly due to the presence of a long-lived isomeric state at 186 keV in the latter that is difficult to separate with R3. The mass precision was therefore sacrificed for higher accuracy. However, if the mass of  $^{124}\text{Ag}$  is remeasured with higher precision, the uncertainties of all other masses will be reduced.

In Fig. 3, the two neutron separation energies ( $S_{2n}$ ) are shown with the updated value for the most neutron-rich

TABLE I. Mass excess from literature and the mass excess of nuclei measured in this work are shown in the second and third column, respectively. Total uncertainties are shown as well as the contribution from the reference mass uncertainty  $\sigma_{m_0}$  and the statistical uncertainty  $\sigma_{stat}$ . The systematic uncertainty  $\sigma_{sys}$  is estimated from the uncertainty of  $T_0$  and the fit parameters  $Length_{3S0}$  and  $TOF_{offset}$  of Eq.(2).

Nucleus	ME <sub>AME20</sub> [keV]	ME <sub>R3</sub> [keV]	$\sigma_{total}$ [keV]	$\sigma_{m_0}$ [keV]	$\sigma_{stat}$ [keV]	$\sigma_{sys}$ [keV]
$^{126}\text{In}$	-77809(4)	-77707	269	254	65	62
$^{125}\text{Cd}$	-73348.1(29)	-73237	320	252	192	40
$^{123}\text{Pd}$	-60430(790)	-60282	265	248	86	40

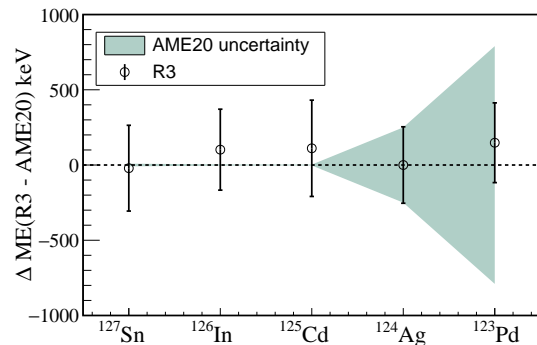


FIG. 2. Mass excess values of nuclei measured at R3 compared to literature values from AME2020 [19]

Pd isotope at  $N=77$ . Nuclear shape deformation before the magic number  $N=82$  was predicted by several models [20–23]. The deformation in this mass region is believed to affect the  $r$ -process abundances before the rise of the  $A=130$  peak. Failure to produce enough material in the  $A=120$  region by several models was thought to be due to the shell quenching at  $N=82$  [23]. However, better description of the deformation in recent nuclear models led to more accurate reproduction of the  $r$ -process abundances before  $A=130$  [24]. The increase in  $S_{2n}$  values can be a signature of such deformation. As can be seen in Fig. 3, the FRDM predicts that nuclear deformation reaches its maximum at the Pd isotopic chain. The new  $S_{2n}$  value of  $^{123}\text{Pd}$  shows a smooth decrease following the trend of the mass surface. Due to still relatively large uncertainty of our mass value, the presence of the deformation cannot be excluded. Based on the estimation of our systematic uncertainties, the mass uncertainty could be reduced to about 100 keV if the mass of  $^{124}\text{Ag}$  is remeasured with a precision of less than 30 keV. It should be noted that the FRDM overestimates the size of the deformation in the Cd isotopic chain, especially when approaching  $N=82$ . Based on experimental masses of Cd isotopes, the deformation in the Ag and Pd isotopic chains might not be as large as that predicted by the FRDM.

We simulate the impact of the mass measurement of  $^{123}\text{Pd}$  in the astrophysical  $r$ -process by employing the

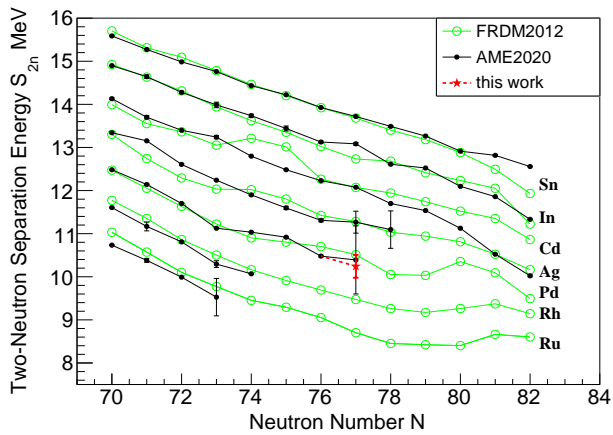


FIG. 3. The two neutron separation energy values ( $S_{2n}$ ) plotted as a function of neutron number from Ru to Sn isotopic chains taken from AME2020 [19]. The  $S_{2n}$  value derived from our new mass value of  $^{123}\text{Pd}$  is shown in red, while predictions of the FRDM are shown by the green line [20].

Portable Routines for Integrated nucleoSynthesis Modeling (PRISM) reaction network [25, 26]. The baseline nuclear physics properties are simulated with FRDM2012 [20, 27–30]. The mass of  $^{123}\text{Pd}$  in the baseline model is also taken from the FRDM2012. Changes to the mass propagate to cross sections and branching ratios in neighboring nuclei as in [9]. We find that the changes in the capture cross sections, and  $\beta$ -delayed neutron probabilities (discussed below) are significant in contrast to other works which do not include these effects [31].

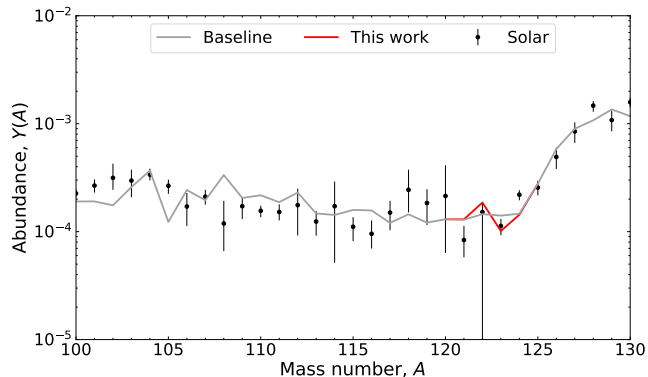


FIG. 4. The local impact (red) of the  $^{123}\text{Pd}$  mass measurement when simulated in the  $r$ -process. The baseline calculation is shown in grey and the solar  $r$ -process residuals in black [32].

Since there are uncertainties in the astrophysical conditions that could produce nuclei in the mass  $A \sim 120$  range, we simulate a set of 20 trajectories with varying neutron-richness from electron fraction of  $Y_e = 0.15$  to  $Y_e = 0.35$  chosen using a procedure similar to that described in [33]. Figure 4 shows the impact of  $^{123}\text{Pd}$

when combining all trajectories together in a weighted sum that best matches the solar  $r$ -process residuals. We find that the neutron capture cross section for  $^{122}\text{Pd}$  decreases by a factor of 2.6 and for  $^{123}\text{Pd}$  increases by a factor of 2.2, while the  $P_{1n}$  value, probability for the  $\beta$ -delayed neutron emission, of  $^{123}\text{Rh}$  increases by 14% with the updated mass, resulting in an effective pileup of material along the  $A = 122$  isobar relative to the baseline. Some conditions enhance this effect, notably  $Y_e = 0.28$  ( $F = 0.61$ ),  $Y_e = 0.29$  ( $F = 1.88$ ),  $Y_e = 0.30$  ( $F = 1.41$ ),  $Y_e = 0.31$  ( $F = 0.99$ ),  $Y_e = 0.32$  ( $F = 0.61$ ) with  $F$  defined as in [34]. As a conclusion, for these conditions there is a larger flow through the  $^{123}\text{Pd}$  nucleus, see also the discussion in [35]. The average impact factor is  $\langle F \rangle = 0.247$ , indicating a local change in the abundances, in line with the prediction of sensitivity studies [34].

In summary, the first application of mass measurements performed by the Rare-RI Ring at the RIBF facility is reported. The most neutron-rich nuclei below the doubly magic nucleus  $^{132}\text{Sn}$  were studied, proving the feasibility for mass measurements of  $r$ -process nuclei at  $N=82$ . The present uncertainty of our measurement can be reduced if the reference mass of  $^{124}\text{Ag}$  is remeasured with higher precision, which will result in a firm conclusion about the presence of nuclear deformation in the Pd isotopic chain. We performed calculations to estimate the impact of the  $^{123}\text{Pd}$  mass measured in the  $r$ -process. We found if our new mass value is used instead of the FRDM value the solar  $r$ -process abundances at  $A=122$  and  $A=123$  are modified, resulting in a better reproduction of the trend in the abundance at these masses. This indicates that the  $r$ -process calculations are very sensitive to masses in this region since a change of  $^{123}\text{Pd}$  mass by just 478keV causes a sizeable effect. This finding highlights the need for high precision mass measurements to address the  $r$ -process in this mass region.

## ACKNOWLEDGMENTS

We are grateful to the RIKEN RIBF accelerator crew and CNS, University of Tokyo for their efforts and supports to operate the RI beam factory. H.F. L. expresses gratitude to the RIKEN International Program Associate. This work was supported by the RIKEN Pioneering Project Funding (“Extreme precisions to Explore fundamental physics with Exotic particles”) and JSPS KAKENHI Grant Nos. 19K03901, 26287036, 25105506, 15H00830, 17H01123, 18H03695, 17K14311. T.M.S. and M.R.M. were supported by the US Department of Energy through the Los Alamos National Laboratory (LANL). LANL is operated by Triad National Security, LLC, for the National Nuclear Security Administration of U.S. Department of Energy (Contract No. 89233218CNA000001). T.M.S. was partly supported by the Fission In R-process Elements (FIRE) Topical Collaboration in Nuclear Theory, funded by the U.S. Depart-

ment of Energy. Yu.A. L. acknowledges support by the European Research Council (ERC) under the European Union’s Horizon 2020 research and innovation program

(grant agreement No 682841 “ASTRUm”). This work is supported by the UK Science and Technology Facilities Council under grant no. ST/P005314/1.

- 
- [1] B. Abbott, Multi-messenger observations of a binary neutron star merger, *Astrophys. J.* **848**, L12 (2017).
- [2] B. P. Abbott, R. Abbott, T. Abbott, F. Acernese, K. Ackley, C. Adams, T. Adams, P. Addesso, R. Adhikari, V. Adya, *et al.*, Gw170817: observation of gravitational waves from a binary neutron star inspiral, *Phys. Rev. Lett.* **119**, 161101 (2017).
- [3] E. M. Burbidge, G. R. Burbidge, W. A. Fowler, and F. Hoyle, Synthesis of the elements in stars, *Rev. Mod. Phys.* **29**, 547 (1957).
- [4] D. Watson, C. J. Hansen, J. Selsing, A. Koch, D. B. Malesani, A. C. Andersen, J. P. Fynbo, A. Arcones, A. Bauswein, S. Covino, *et al.*, Identification of strontium in the merger of two neutron stars, *Nature* **574**, 497 (2019).
- [5] D. M. Siegel, J. Barnes, and B. D. Metzger, Collapsars as a major source of r-process elements, *Nature* **569**, 241 (2019).
- [6] A. P. Ji, A. Frebel, A. Chiti, and J. D. Simon, R-process enrichment from a single event in an ancient dwarf galaxy, *Nature* **531**, 610 (2016).
- [7] K. Farouqi, F.-K. Thielemann, S. Rosswog, and K.-L. Kratz, Correlations of r-process elements in very metal-poor stars as clues to their nucleosynthesis sites (2021), arXiv:2107.03486 [astro-ph.SR].
- [8] R. Surman, J. Beun, G. C. McLaughlin, and W. R. Hix, Neutron capture rates near  $a = 130$  that effect a global change to the r-process abundance distribution, *Phys. Rev. C* **79**, 045809 (2009).
- [9] M. R. Mumpower, R. Surman, D. L. Fang, M. Beard, P. Möller, T. Kawano, and A. Aprahamian, Impact of individual nuclear masses on r -process abundances, *Phys. Rev. C* **92**, 035807 (2015), arXiv:1505.07789 [nucl-th].
- [10] B. Côté, K. Belczynski, C. L. Fryer, C. Ritter, A. Paul, B. Wehmeyer, and B. W. O’Shea, Advanced ligo constraints on neutron star mergers and r-process sites, *Astrophys. J.* **836**, 230 (2017).
- [11] K. Hotokezaka, P. Beniamini, and T. Piran, Neutron star mergers as sites of r-process nucleosynthesis and short gamma-ray bursts, *International Journal of Modern Physics D* **27**, 1842005 (2018).
- [12] D. Nagae, S. Omika, Y. Abe, Y. Yamaguchi, F. Suzuki, K. Wakayama, N. Tadano, R. Igosawa, K. Inomata, H. Arakawa, *et al.*, First demonstration of mass measurements for exotic nuclei using rare-ri ring, in *Proceedings of 10th International Conference on Nuclear Physics at Storage Rings (STOR’17)* (2021) p. 011014.
- [13] N. Fukuda, T. Kubo, T. Ohnishi, N. Inabe, H. Takeda, D. Kameda, and H. Suzuki, Identification and separation of radioactive isotope beams by the bigrips separator at the riken ri beam factory, *Nucl. Instrum. Methods Phys. Res. Sect. B* **317**, 323 (2013), xVIth International Conference on ElectroMagnetic Isotope Separators and Techniques Related to their Applications, December 2–7, 2012 at Matsue, Japan.
- [14] Y. Yamaguchi *et al.*, Isochronous mass spectrometry with pre-identified single event (2021).
- [15] D. Nagae, Y. Abe, S. Okada, and *et. al*, Development and operation of an electrostatic time-of-flight detector for the rare ri storage ring, *Nucl. Instrum. Methods Phys. Res., Sect. A* **986**, 164713 (2021).
- [16] A. Abe, Y. Yamaguchi, M. Wakasugi, D. Nagae, F. Suzuki, and for the Rare RI Ring collaboration, Update of the particle selection system for the rare ri ring experiments, *RIKEN Accel. Prog. Rep.* **52**, 15 (2019).
- [17] A. Ozawa, T. Uesaka, M. Wakasugi, and the Rare-RI Ring Collaboration, The rare-RI ring, *Prog. Theor. Exp. Phys.* **2012** (2012), 03C009.
- [18] S. Naimi, H. Li, Y. Abe, and *et. al*, Experimental challenges of the first mass measurement campaign at the rare-ri ring, *Journal of Physics: Conference Series* **1643**, 012058 (2020).
- [19] M. Wang, W. Huang, F. Kondev, G. Audi, and S. Naimi, The ame 2020 atomic mass evaluation (ii). tables, graphs and references, *Chin. Phys. C* **45**, 030003 (2021).
- [20] P. Möller, A. J. Sierk, T. Ichikawa, and H. Sagawa, Nuclear ground-state masses and deformations: FRDM(2012), *Atomic Data and Nuclear Data Tables* **109**, 1 (2016), arXiv:1508.06294 [nucl-th].
- [21] H. Koura, T. Tachibana, M. Uno, and M. Yamada, Nucleonic mass formula on a spherical basis with an improved even-odd term, *Progress of theoretical physics* **113**, 305 (2005).
- [22] S. Goriely, Further explorations of skyrme–hartree–fock–bogoliubov mass formulas. xv: The spin–orbit coupling, *Nuclear Physics A* **933**, 68 (2015).
- [23] J. Pearson, R. Nayak, and S. Goriely, Nuclear mass formula with bogolyubov-enhanced shell-quenching: application to r-process, *Phys. Lett. B* **387**, 455 (1996).
- [24] K.-L. Kratz, K. Farouqi, and P. Moller, A high-entropy-wind r-process study based on nuclear-structure quantities from the new finite-range droplet model frdm(2012), *Astrophys. J.* **792**, 6 (2014).
- [25] T. M. Sprouse, R. Navarro Perez, R. Surman, M. R. Mumpower, G. C. McLaughlin, and N. Schunck, Propagation of statistical uncertainties of Skyrme mass models to simulations of r -process nucleosynthesis, *Phys. Rev. C* **101**, 055803 (2020), arXiv:1901.10337 [nucl-th].
- [26] T. M. Sprouse, M. R. Mumpower, and R. Surman, Following nuclei through nucleosynthesis: A novel tracing technique, *Phys. Rev. C* **104**, 015803 (2021), arXiv:2008.06075 [nucl-th].
- [27] P. Möller, A. J. Sierk, T. Ichikawa, A. Iwamoto, and M. Mumpower, Fission barriers at the end of the chart of the nuclides, *Phys. Rev. C* **91**, 024310 (2015).
- [28] M. R. Mumpower, T. Kawano, and P. Möller, Neutron- $\gamma$  competition for  $\beta$  -delayed neutron emission, *Phys. Rev. C* **94**, 064317 (2016), arXiv:1608.01956 [nucl-th].
- [29] M. R. Mumpower, T. Kawano, T. M. Sprouse, N. Vassh, E. M. Holmbeck, R. Surman, and P. Möller,  $\beta$ -delayed Fission in r-process Nucleosynthesis, *Astrophys. J.* **869**, 14 (2018), arXiv:1802.04398 [nucl-th].

- [30] P. Möller, M. R. Mumpower, T. Kawano, and W. D. Myers, Nuclear properties for astrophysical and radioactive-beam applications (II), *Atomic Data and Nuclear Data Tables* **125**, 1 (2019).
- [31] D. Martin, A. Arcones, W. Nazarewicz, and E. Olsen, Impact of Nuclear Mass Uncertainties on the r Process, *Phys. Rev. Lett.* **116**, 121101 (2016), arXiv:1512.03158 [nucl-th].
- [32] M. Arnould, S. Goriely, and K. Takahashi, The r-process of stellar nucleosynthesis: Astrophysics and nuclear physics achievements and mysteries, *Phys. Rep.* **450**, 97 (2007), arXiv:0705.4512 [astro-ph].
- [33] E. M. Holmbeck, T. M. Sprouse, M. R. Mumpower, N. Vassh, R. Surman, T. C. Beers, and T. Kawano, Actinide production in the neutron-rich ejecta of a neutron star merger, *Astrophys. J.* **870**, 23 (2018).
- [34] M. R. Mumpower, R. Surman, G. C. McLaughlin, and A. Arahamian, The impact of individual nuclear properties on r-process nucleosynthesis, *Prog. Part. Nucl. Phys.* **86**, 86 (2016), arXiv:1508.07352 [nucl-th].
- [35] M. R. Mumpower, G. C. McLaughlin, and R. Surman, Influence of neutron capture rates in the rare earth region on the r-process abundance pattern, *Phys. Rev. C* **86**, 035803 (2012), arXiv:1204.0437 [nucl-th].
- [36] R. Knöbel, M. Diwisch, H. Geissel, Y. A. Litvinov, Z. Patyk, W. Plaß, C. Scheidenberger, B. Sun, H. Weick, F. Bosch, *et al.*, New results from isochronous mass measurements of neutron-rich uranium fission fragments with the frs-esr-facility at gsi, *Eur. Phys. J. A* **52**, 1 (2016).
- [37] I. U. Roederer, J. E. Lawler, J. J. Cowan, T. C. Beers, A. Frebel, I. I. Ivans, H. Schatz, J. S. Sobeck, and C. Sneden, Detection of the second r-process peak element tellurium in metal-poor stars, *Astrophys. J. Lett.* **747**, L8 (2012).
- [38] I. U. Roederer, J. E. Lawler, J. S. Sobeck, T. C. Beers, J. J. Cowan, A. Frebel, I. I. Ivans, H. Schatz, C. Sneden, and I. B. Thompson, New hubble space telescope observations of heavy elements in four metal-poor stars, *Astrophys. J. Suppl. Ser.* **203**, 27 (2012).
- [39] E. Anders and M. Ebihara, Solar-system abundances of the elements, *Geochimica et Cosmochimica Acta* **46**, 2363 (1982).
- [40] S. Bisterzo, R. Gallino, O. Straniero, S. Cristallo, and F. Käppeler, The s-process in low-metallicity stars – ii. interpretation of high-resolution spectroscopic observations with asymptotic giant branch models, *Monthly Notices of the Royal Astronomical Society* **418**, 284 (2011).